

Influence of the Drying Route on the Depolymerization and Properties of Chitosan

Mabel K. Arantes,¹ Cristie L. Kugelmeier,¹ Lucio Cardozo-Filho,² Marcos R. Monteiro,³ Clayton R. Oliveira,³ Helton J. Alves¹

¹ Laboratory of Catalysis and Biofuel Production (LabCatProBio), Biofuels Technology Course, Federal University of Paraná (UFPR - Setor Palotina), R. Pioneiro, 2153, Jardim Dallas, 85950-000 Palotina, Parana, Brazil

² Department of Chemical Engineering (DEQ), State University of Maringá (UEM), Av. Colombo, 5790, Jardim Universitário, 87020-900 Maringá, Parana, Brazil

³ Materials Characterization and Development Center (CCDM/DEMa), Federal University of São Carlos (UFSCar), Rod. Washington Luis, km 235, 13565-905 São Carlos, Sao Paulo, Brazil

In this work, a chitosan sample with a high degree of deacetylation (DD >95%) obtained from freshwater shrimp shells was subjected to drying processes in an electric oven and by supercritical CO₂. The results indicated that drying chitosan particles with supercritical CO₂ resulted in a very significant increase in specific surface area and pore volume, and also increased the material's crystallinity index. This drying route led to a more than 10-fold reduction in viscosimetric molecular weight (from 35.3 to 3.0 kDa), indicating that the physical drying process caused the chitosan to depolymerize, which usually occurs by enzymatic and chemical methods, according to the literature. Low molecular weight chitosan is essential for some applications in the field of biomedicine (drug delivery for example); hence, drying via the CO₂ route can be considered a promising technique for the production of high value-added materials with applications in this area. POLYM. ENG. SCI., 00:000-000, 2014. © 2014 Society of Plastics Engineers

INTRODUCTION

The deacetylation of chitin—a polysaccharide occurring abundantly in nature and extracted commercially from fish industry waste, such as crab and shrimp shells, among other sources—yields chitosan. Chitosan is a biopolymer which has several possible applications due, among other factors, to the properties conferred on it by the amino groups ($-\text{NH}_2$) obtained by the conversion of acetamide groups ($-\text{NHCOCH}_3$) [1] (Fig. 1). The industrial and technological applications of chitosan have been exploited for decades, for example, in the production of cosmetics, drugs, and medicines, food additives, semipermeable membranes, in the development of biomaterials used in Schiff base reactions to produce salicylaldehyde derivatives [1], as a drug delivery agent for the human body [2, 3], and in the textile industry as an alternative for treating effluents containing dyes [4].

Shrimp farming has received a great deal of attention worldwide, mainly because of the growing market demand and high commercial value attained by the product. Therefore, shrimp waste is widely available and has even become an environmental problem. According to FAO (Food and Agriculture Organiza-

tion of the United Nations) [5], the worldwide production of farmed shrimp dropped to 2.5 million tons in 2011, and it is known that about 40% of this product (1 million tons) consists of wastes containing high levels of chitin (15–20%), proteins (25–40%), inorganic salts (ash 40–55%), and carotenoid pigments (about 15%) [6]. Therefore, not only do these wastes contaminate the environment but also tons of products of great economic potential are being wasted. This type of waste is abundantly available in Brazil's coastal regions, but less so in the interior of the country. However, is particularly abundant in the western region of the state of Paraná (Brazil) due to the growing combined production of freshwater shrimp and tilapia in ponds. This fact, allied to the promising aspects of chitosan applications in various areas, motivated us to produce this biopolymer in our laboratory with a high degree of deacetylation (DD).

The higher the DD of chitosan the greater its chemical influence on some of its properties, such as hydrophobicity, ability to undergo crosslinking by crosslinking agents, and its solubility and viscosity in solutions. In addition to the DD, the molar mass and crystallinity of chitosan are important factors for its application, since they affect most of the characteristics of the biopolymer. The DD of commercial chitosan usually varies from 70 to 95%, with a molecular weight in the range of 10 to 10³ kDa and a semicrystalline structure.

The influence of the molar mass of chitosan on its properties and applications can be exemplified in the biomedical field, where it is increasingly used in drug delivery systems. These systems require low molar mass biopolymer, since solutions of low viscosity are essential [3]. Studies have shown that molecular weights exceeding 50 kDa increase the viscosity of solutions, often rendering them unviable [2]. For gene delivery systems, studies have shown that low molecular weight and high charge density chitosan exhibited a stronger binding affinity to DNA than high molecular weight chitosan [7]. Researchers relate also that low molar mass chitosan exhibits higher biological activity, including bactericidal activity, hypolipidemic and hypocholesterolemic effects [8], and stimulation of murine peritoneal macrophages that kill tumor cells [9]. Several depolymerization methods have been developed in an attempt to reduce the molar mass of chitosan, and hence the viscosity of its solutions, including prolonged acid treatment [10], enzymatic degradation [8], ultraviolet-irradiated oxygen [11], and others.

When chitin is processed to obtain chitosan, the drying step must be carried out with a view to preserving the product's

Correspondence to: H. J. Alves; e-mail: helquimica@gmail.com

DOI 10.1002/pen.24038

Published online in Wiley Online Library (wileyonlinelibrary.com).

© 2014 Society of Plastics Engineers

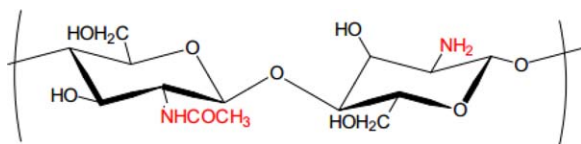


FIG. 1. Chemical structure of chitosan: 2-amino-2-deoxy-D-glucose and 2-acetamido-2-deoxy-D-glucose copolymer. [Color figure can be viewed in the online issue, which is available at wileyonlinelibrary.com.]

original characteristics or else to make modifications of interest, as well as to ensure adequate moisture content for purposes of storage and sale [12]. Chitosan can be dried by several methods, including: oven drying; lyophilization [13]; spray drying [14], and the method under study here, using supercritical CO₂ (SAS—Supercritical Antisolvent Precipitation) [15]. Oven drying is a method that promotes direct particle-fluid contact, with high rates of heat and mass transfer. Industrially, chitosan is dried in tray dryers, bed-dryers, thin film dryers and spouted bed dryers for drying suspensions, as well as pastes and solutions [16]. In the freeze drying method (lyophilization), the solvent (usually water) and/or a suspension dries by crystallization at low temperatures in a vacuum chamber that allows for the removal of solvent by sublimation at temperatures of -10°C or lower [13]. In spray drying, which involves temperatures of 150 to 600°C, small droplets of suspension formed by a rotary disc (atomizer) dry rapidly, and the dried material is removed by exhaustion of the particles [14].

A material is in the supercritical fluid state when it is above its critical temperature (T_c) and critical pressure (P_c), which, in the case of CO₂, is achieved under conditions of $T_c = 31^{\circ}\text{C}$ and $P_c = 73.8$ bar [17]. To dry a material by this method, the drying apparatus consists basically of a CO₂ cylinder, valves, a thermostatic bath, a syringe pressure pump, an agitation system, resistive heating elements, and pressure and temperature displays [18]. This is an attractive method for obtaining particulate materials with controlled properties such as morphology, size, and crystallinity, which can be controlled by adjusting the temperature and pressure used in the process. The reuse of solvent is a major advantage of the process since it ensures its rational use, generating savings in drying, as well as avoiding its discharge in the form of gases into the environment. A particular advantage of this technique is its adaptability to continuous operations, which favors the large scale production of particles.

To evaluate the influence of the drying technique, García-Bermejo et al. [19] compared freeze drying and supercritical conditions when drying chitosan microspheres using the Mailard reaction, which consists of producing chitosan-carbohydrate derivatives to increase the solubility of the biopolymer in water. These authors observed a significant difference in specific surface area ($111\text{ m}^2\text{ g}^{-1}$ by supercritical CO₂ drying vs. $3.60\text{ m}^2\text{ g}^{-1}$ by freeze drying). Thakhiew et al. [20] found that the crystallinity index (I_{cr}) can also be altered significantly by the drying conditions applied to chitosan films. Crystallinity, which varies according to the source of chitin and can also be altered during processing of the biopolymer, controls the accessibility to its sorption sites and its diffusion properties. The crystallinity of chitosan diminishes when it is solubilized, but the material's final crystallinity is determined by the subsequent drying process. In this regard, Jaworska et al. [21] demonstrated that the

crystallinity of chitosan is reduced upon solubilization and drying at 60°C, and that this reduction is even higher in freeze drying. Srinivasa et al. [22] also observed this phenomenon upon comparing three chitosan film drying methods: in ambient air ($T \sim 27^{\circ}\text{C}$), in an electric oven (80 to 100°C), and by infrared radiation (80 to 100°C). They reported that radiation drying led to a higher crystallinity index than the other methods, suggesting an increase in hydrophobic interactions in response to increasing temperature.

Various methods were employed here to dry samples from the same batch of chitosan, aiming to identify the effect of this unit operation on their physicochemical properties, particularly with respect to viscosimetric molar mass, crystallinity and porosity. This work differs from others published in the literature in that it uses supercritical CO₂ fluid to dry chitosan in the form of powder (irregular particles) instead of in microspheres, which is the normal route, and investigates the effect of the drying step on the depolymerization of chitosan.

MATERIALS AND METHODS

Isolation of Chitin and Preparation of Chitosan

Chitin was extracted from the exoskeletons of *Macrobrachium rosenbergii* freshwater prawn farmed in the western region of the state of Paraná, Brazil. Initially, the shells were washed under running water and sun-dried, after which they were crushed, dry ground in a ball mill, and sieved until they passed completely through a sieve with 63 μm openings. The resulting material was demineralized and deproteinized according to the method described by Tolaimate et al. [6]. The chitin deacetylation reaction was carried out by preparing a mixture of chitin and a solution of NaOH 50% (m/V) in a proportion of 2.5% (w/v), which was refluxed at 100°C for 10 h. The reaction product was washed to neutralize the pH and then dried at 60°C for 24 h.

Preparation of the Chitosan Sample for Drying Tests

Three chitosan drying procedures were tested: two oven drying procedures for the samples identified as Q1 and Q2, and supercritical CO₂ drying for sample Q3. In each case, preparation of the sample consisted of solubilizing chitosan in a solution of 0.1 M of hydrochloric acid, in a proportion of 0.4% (w/v), followed by drip precipitation in a solution of 2.0 M of NaOH under stirring. The precipitated material was filtered and washed with solutions of absolute ethanol at increasing concentrations (10, 30, 50, 70, 90, and 100%) at 15 min intervals for each wash.

Chitosan Drying Techniques

Sample Q1 was spread onto glass surfaces (Petri dishes), forming a layer about 4 mm thick, and was oven-dried at 60°C for 24 h. The resulting material was then comminuted in a mortar until it passed through a 63 μm (230 mesh) particle size sieve. Sample Q2 was dried in two steps. The first step consisted of spreading the sample on a glass surface to form a fine layer of 1 mm thick, which was dried for 10 min at 60°C. Then, the film was removed with a spatula and dried at 60°C for 24 h. The resulting material was then comminuted in a mortar (similar to Q1). Sample Q3 was dried under supercritical CO₂ conditions

TABLE 1. Drying conditions and physicochemical properties of samples Q1, Q2, and Q3.

Sample	Drying		Crystallinity			Porosity			Viscosity ^a		
	Time (h)	Temperature (°C)	Pressure (bar)	I_{cr} (%) ^b	D_{ap} (Å) ^c	Specific surface area (m ² g ⁻¹)	Pore volume (cm ³ g ⁻¹)	Pore size (Å)	Deacetylation DD (%)	$[\eta]$ (mL g ⁻¹)	M_V^d (kDa)
Q1	24	60	1.013	57	29.2	1.07	0.0055	98.2	96	217.3 ± 1.5	35.3
Q2	First: 0.17 Second: 24 ^e	60	1.013	60	33.1	16.7	0.0469	56.2	97	127.4 ± 1.0	17.6
Q3	2	32	74.0	64	39.9	202.1	1.489	14.7	96	32.9 ± 1.2	3.0

^aK = 0.076 and $\alpha = 0.76$ (solvent 0.3M HAc /0.2M NaAc, at 25°C) [23].

^bThe calculation was performed using I_c and I_a , corresponding to $2\theta = 19.35^\circ$ and 12.70° , respectively.

^cThe calculation was based on the data of the main peak at $2\theta = 19.35^\circ$.

^dCalculating M_V was determined using the average value of $[\eta]$.

^eTwo-stage drying.

(74 bar, 32°C) for 2 h, using the SAS method [18]. Table 1 describes the set of drying conditions applied to the three samples.

Physicochemical Characterization of Chitin and Chitosan

The efficiency of the demineralization (DM) and deproteinization (DP) steps on the isolation of chitin was evaluated based on ash content, which was determined by burning the samples in a crucible at 600°C in an electric muffle furnace, while the protein content was measured by subjecting the samples to the standard biuret protein assay and the Kjeldahl method, before and after the processes [6].

The average degree of acetylation (DA) of chitosan was determined by ¹H NMR, using a Bruker Avance III spectrometer and 9.4 Tesla, in the following experimental conditions: 400 MHz for hydrogen frequency (SWH), experimental temperature of 323 K, 16 scans (ns), wait time of 10 s (d1), acquisition time of 6.83 s (aq), and 65,536 data points (td). The %DA and %DD were calculated as described by Santos et al. [24].

The chitosan powder samples were prepared by mixing with KBr in a concentration of 1% (w/w), homogenized in a mortar, pelletized, and analyzed by Fourier transform infrared (FTIR) spectroscopy. The spectra were obtained in the range of 4000 to 500 cm⁻¹ with resolution of 4 cm⁻¹ in 21 scans (Bomem MB Series FTIR).

Thermogravimetric and derivative thermogravimetry (TGA/DTA) curves were obtained on a TA Instruments Q-500 module, at a nitrogen flow of 50 mL/min, heating rate of 10°C/min, and maximum temperature of 600°C, for the thermal analysis of the chitosan samples, using about 10 mg of sample. To check the morphology and size of the particles formed after each drying method, an analysis by scanning electron microscopy was performed on a FEI Quanta 400. The semicrystalline structure of the chitosan samples was analyzed by X-ray diffraction (XRD), using a Rigaku Multiflex diffractometer (Cu K α radiation with $\lambda = 1.54$ Å, 40 kV voltage and 40 mA current), with continuous scanning in the interval of $5^\circ < 2\theta < 50^\circ$ and a scan speed of 1°/min. The crystallinity index (I_{cr}) of the samples was determined based on an analysis of the diffraction patterns, using Eq. 1 [25],

$$I_{cr} = \left(\frac{I_c - I_a}{I_c} \right) \cdot 100 \quad (1)$$

where I_{cr} is the crystallinity index; I_c represents the intensity of the signal corresponding to the crystalline regions; and I_a repre-

sents the intensity of the signal corresponding to the amorphous regions. Based on these results, it was also possible to estimate the value of the apparent diameter of the crystallites (D_{ap}) in Å, using Scherrer's equation (Eq. 2) [26],

$$D_{ap} = \frac{K\lambda}{\beta_0 \cos \theta} \quad (2)$$

where D_{ap} is the average diameter of the crystallites (Å) in the direction perpendicular to the plane (110); β_0 corresponds to the width of the peak of the main signal in the crystalline regions at half maximum intensity (radians); K is a constant (value 0.9); θ is half the Bragg angle of the most intense signal (radians); and λ is the wavelength of the radiation applied (Å). To identify the predominant type of porous structure in the chitosan samples and determine the pore volume, adsorption/desorption isotherms were recorded at the liquid nitrogen temperature, using a Quantachrome Surface Area Analyzer (nitrogen physisorption method—BET). The BJH (Barret–Joyner–Halenda) method was used to determine the pore volume. The chitosan powder samples were treated under vacuum at 150°C for 6 h and their specific surface areas, pore volume and pore size were estimated by means of the BET equation, using $P/P_0 \leq 0.3$ [27].

To determine the molar mass by viscometry, a chitosan solution 0.1% (m V⁻¹) in 0.3 M acetic acid was stirred constantly for 24 h, after which it was diluted (2x) with 0.2 M sodium acetate and stirred for another 24 h. The samples were filtered through an 80 μ m membrane and aliquots of 15 mL were transferred to an Ubbelohde glass capillary ($\varphi = 0.53$ mm) thermostated at $25^\circ\text{C} \pm 0.1^\circ\text{C}$ for serial dilution. The concentrations used here ranged from 0.31 to 0.55 mg mL⁻¹. The flow times were determined using an AVS-350 viscometer coupled to an AVS 20 automatic diluter system, both from Schott-Geräte. The flow times correspond to the average of three independent determinations with variations of less than 0.5%. The relationship between the intrinsic viscosity and the molecular weight of the polymer is established by the Mark–Houwink–Sakurada equation [23] (Eq. 3),

$$[\eta] = K\bar{M}_V^\alpha \quad (3)$$

where $[\eta]$ is the intrinsic viscosity (dL g⁻¹), M_V is the average viscosimetric molar mass, and K and α are constants for a given polymer-solvent system, which, in the case of chitosan, varies according to the DA as well as molecular weight range.

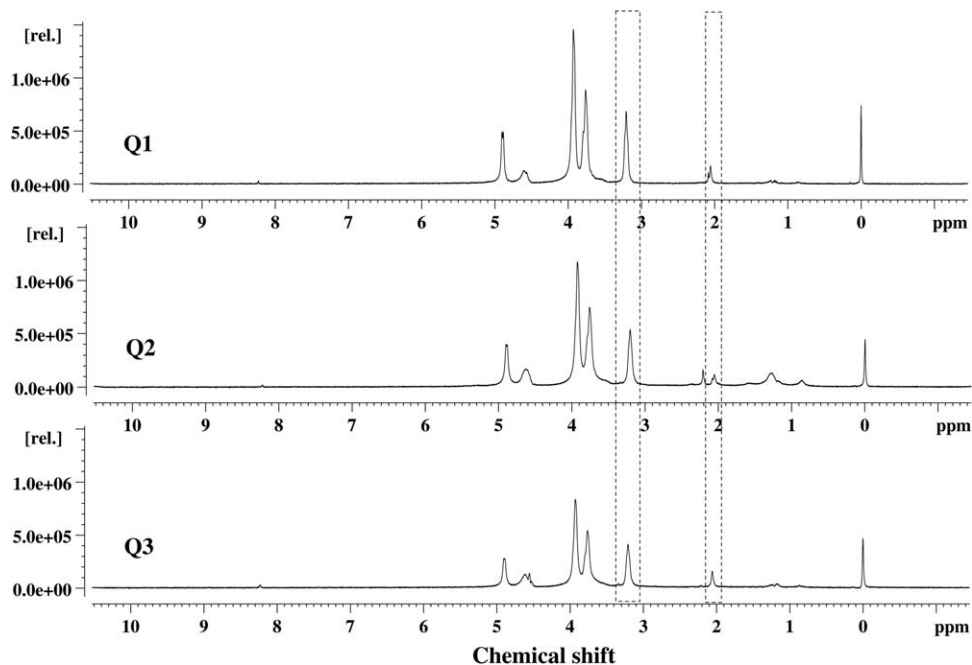


FIG. 2. ^1H NMR spectra of samples Q1, Q2, and Q3. The dashed lines in the regions of 3.30 to 3.10 ppm and of 2.08 to 2.00 ppm refer to the hydrogens of the amino and acetyl groups, respectively.

RESULTS AND DISCUSSION

Characterization of Chitin

Chitin is a constituent of shrimp shells and its isolation consists of the extraction of the minerals and proteins that also make up the shell structure. Thus, the main parameters to be evaluated with respect to chitin are the efficiency of the DM) and DP steps after acid and alkaline treatments, and the yield in chitin. In this study, the %DM and %DP were evaluated and showed an efficiency of 99.8 and 99.9%, respectively. The chitin recovery from Shells shrimp was 20% (m m^{-1}), which falls within the range of values for chitin content in shrimp shells reported in the literature [6]. The choice of DM and DP methods (concentration of solutions, temperature and time) took into account that the native structure of the biopolymer should be preserved, minimizing degradation or partial deacetylation, although it is known that acid and base treatments cause degradation of the biopolymer, even prior to the deacetylation reaction that will follow.

Characterization of Chitosan Subjected to Different Drying Methods

Average Degree of Deacetylation and Average Viscosimetric Molar Mass. Starting from the complete removal of proteins and minerals, the deacetylation method chosen in this work took into account the results reported in the literature for the deacetylation of chitin isolated from shrimp with a DD higher than 70% [6, 28], keeping in mind that different sources of chitin may require different deacetylation reaction times to reach the same DD. After purification and drying process of the chitosan the material was characterized by ^1H NMR, resulting in the spectra depicted in Fig. 2. In this figure, the regions of interest are those from 3.30 to 3.10 ppm and from 2.08 to 2.00 ppm, which are relative to the hydrogens of the amino and acetyl groups, respectively, for which the peak areas were determined

for the determination of the %DA. Based on the %DA, the %DD was calculated for samples Q1, Q2, and Q3, which indicated that the chitosan was highly deacetylated (Table 1).

The influence of the drying process on the molar mass of chitosan was measured by viscometry, which, albeit not an absolute method, is one of the techniques most commonly employed to determine the molar mass of polymers. The concentrations of chitosan solutions prepared for viscosimetric measurements were tested and defined to meet the ideal condition of the optimal range of relative viscosity (1.1 to 1.5) and a flow time above 100 s, which are relevant factors for reliable determinations [29].

The intrinsic viscosity $[\eta]$ and viscosimetric molar mass (M_v) (Table 1) of chitosan after the three drying methods reveals a very interesting characteristic. When the drying was performed via supercritical CO_2 (sample Q3), the molar mass decreased approximately 10-fold (depolymerization), while oven-drying led to a twofold decrease when the thickness of the film material was reduced (Q2) and the film was subjected to the two-step drying method. The following assumptions may help explain the effect of drying on chitosan depolymerization in comparison with the conditions used for sample Q1 [30–32]:

- i. Sample Q2: because the chitosan film was thinner, its water removal rate was higher in the first drying step and the temperature exerted a stronger effect, causing an increase in the thermal vibration of C-C bonds in the polymer main chain, resulting in depolymerization;
- ii. Sample Q3: the circular motion in drying via supercritical CO_2 under high pressure can tension the material's polymer chains, resulting in its depolymerization.

Thus, it is reasonable to suggest that the drying chitosan via supercritical CO_2 technique is useful for obtaining this biopolymer

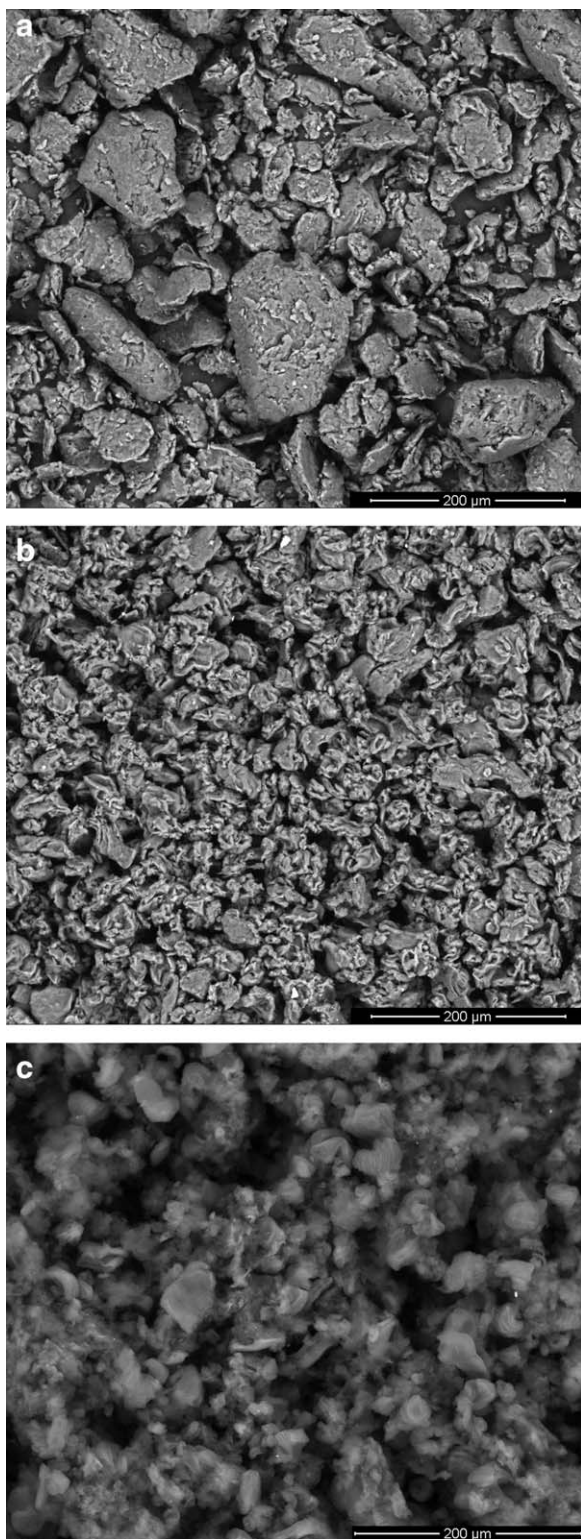


FIG. 3. Micrographs of samples (a) Q1, (b) Q2, and (c) Q3.

with a low molar mass since MV value obtained after this process corresponds to commercial chitosan considered the low molar mass has, for example, 5, 10, and 20 kDa [2], or even higher values. Another favorable aspect regarding the use of supercritical CO₂ is that it is a simple technique when compared with other processes involved in chitosan depolymerization aimed at obtain-

ing low molar mass, including chemical, physical, and enzymatic processes. A few examples of such processes are: acid treatment and microwave radiation, resulting in a reduction from 10 to 3 kDa, but with the disadvantage of high cost and residual acidity [33]; irradiation at different temperatures in acid medium for 35 days to achieve a reduction from 71 to 21 kDa [10]; and enzymatic reactions using proteases such as papain, a cysteine protease, keeping in mind, however, that a high level of pyrogenicity may occur due to the presence of proteins mixed with the end product [8], as the focus of application is biomedical. Thus, since the CO₂ drying technique leaves no residue in the end product, is fast and takes place at low temperatures, it may be considered advantageous because it consists of a physical method that allows for the depolymerization of chitosan, which is desired, for instance, for use in the field of biomedicine.

Surface Characteristics of Particles. As can be seen in the micrographs in Fig. 3, the particle size and surface characteristics were significantly decreased by SAS when drying with supercritical CO₂, (Fig. 3c). The particles of sample Q3 forms have more homogeneous shapes and less irregular surfaces than those of samples Q1 and Q2. A comparison of the particles of samples Q1 (Fig. 3a) and Q2 (Fig. 3b) reveals that the rapid drying of a thin film of sample Q2 resulted in particles with regular sizes, smoother surfaces and larger specific surface area (Table 1).

Crystallinity Index (I_{cr}). Chitosan has a semicrystalline profile due to strong intra- and intermolecular interactions, characterized by hydrogen bridges formed between the amino, hydroxyl, amide, and other functional groups that are present in the molecule.

The XRD analysis revealed peaks characteristic of semicrystalline chitosan (Fig. 4), as described by Mekahlia and Bouzid [34]. The main crystalline peaks visible in the diffractograms of samples Q1, Q2, and Q3 are located at $2\theta = 9.42^\circ$, 19.35° , and 26.45° .

As the chitosan analyzed in this paper comes from shrimp shells, the isolated chitin must be of α -chitin type [6]. The XRD patterns of samples Q1, Q2, and Q3 show the presence of the peak at approximately 10° , corresponding to the (010) planes, which in turn are attributed to orthorhombic crystals derived from the α -chitin structure. The most intense crystalline peak, which is visible at approximately 20° , corresponds to the (110) and (020) planes.

In the diffractograms in Fig. 4, also note that the three samples have very similar characteristics. However, the crystalline peaks of sample Q1 are broader and less intense, while those of sample Q3 are better defined and more intense.

The crystallinity index (I_{cr}) and the average crystallite diameter (D_{ap}) were determined using *Eqs. 1* and *2* and are listed in Table 1. The crystallinity and crystallite diameter varied as follows: $Q1 < Q2 < Q3$. The hypotheses proposed to explain the differences observed are as follows:

- i. In sample Q1, although complete oven drying took place at 60°C for 24 h, there was a very fast loss of much of the volume of solvent at the beginning of the drying cycle (in less than 1 h), which impaired the crystallization (nucleation) and growth of crystallites.

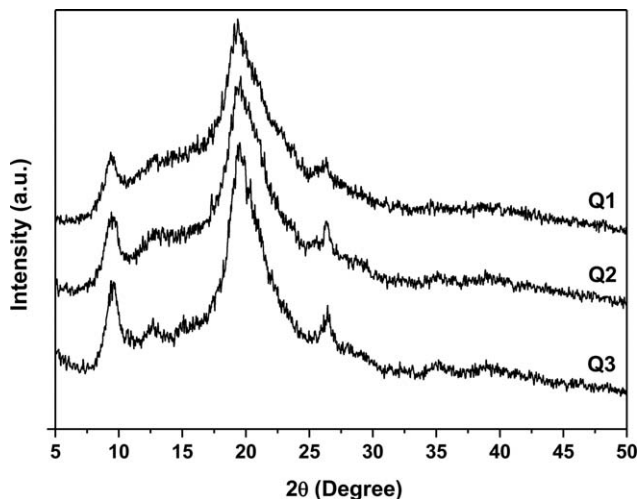


FIG. 4. Diffractograms of samples Q1, Q2, and Q3.

- ii. The solvent exit rate in sample Q2 is faster than in sample Q1 (the same temperature of 60°C has a stronger effect on a thinner layer,) which hinders crystallite growth. However, upon returning to the oven, the new heating cycle enables the growth of crystallites in the particles, which are now smaller, solid and already nucleated, and hence, an increase in crystallinity.
- iii. The effective water exit rate in sample Q3 is slower than in sample Q2 (2 h in SAS), which, allied to the lower temperature, favors crystallite growth and greater crystallization.

FTIR Analysis. The peaks corresponding to the types of bonds in chitosan, which were evaluated by FTIR, showed that there were no significant variations arising from the drying process. The infrared spectra (Fig. 5) showed bands characteristic of chitosan, as reported in the literature [23]: OH axial stretching band between 3440 and 3480 cm^{-1} , which appears superimposed on the N—H stretching band; C=O axial deformation of amide I (between 1661 and 1671 cm^{-1}); N—H angular deformation (between 1583 and 1594 cm^{-1}); CH_3 symmetric angular

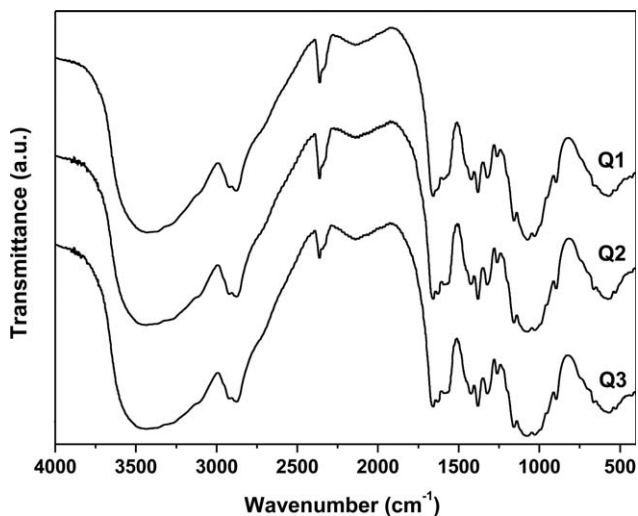


FIG. 5. FTIR spectra of samples Q1, Q2, and Q3.

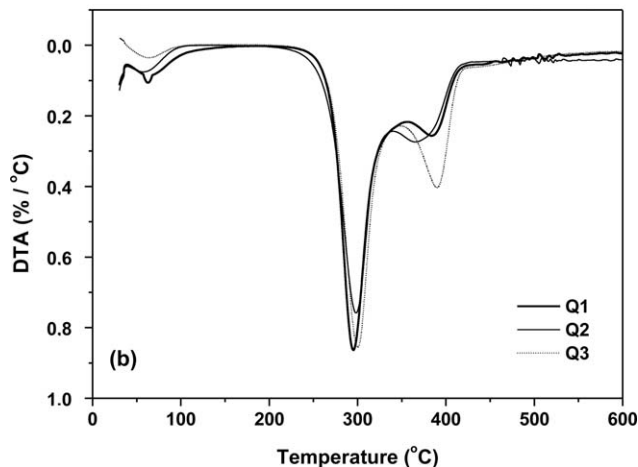
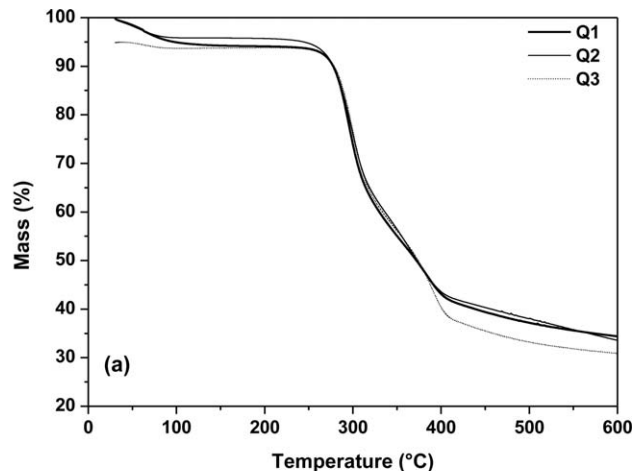


FIG. 6. Thermograms of samples Q1, Q2, and Q3: (a) TGA and (b) DTA.

deformation (between 1380 and 1383 cm^{-1}); —CN axial deformation of amide (at around 1425 cm^{-1}), and —CN axial deformation of amino groups (from 1308 and 1380 cm^{-1}), as well as bands of polysaccharide structures in the region of 890–1156 cm^{-1} . Similar results were also reported by Junior & Mansur [35] and Brugneroto et al. [36].

Thermal Stability. The thermal analysis of the chitosan samples revealed the main temperatures at which the material's decomposition and weight loss occur (Fig. 6a and b). The thermograms indicated that the residual water and ethanol used for washing the chitosan samples before drying volatilized at up to 100°C. Note that the samples showed minimal weight loss up to approximately 200°C.

The samples are very similar with respect to thermal degradation of the biopolymer (200–330°C), and the maximum degradation temperature of the samples (recorded at the minimum point in the first derivative) is virtually the same (300°C).

The most significant difference between the samples is the higher weight loss of sample Q3 in the second thermal event recorded between 330 and 420°C. Because the DD of sample Q3 is lower than that of the other samples, the higher weight loss in this temperature range can be attributed to the greater

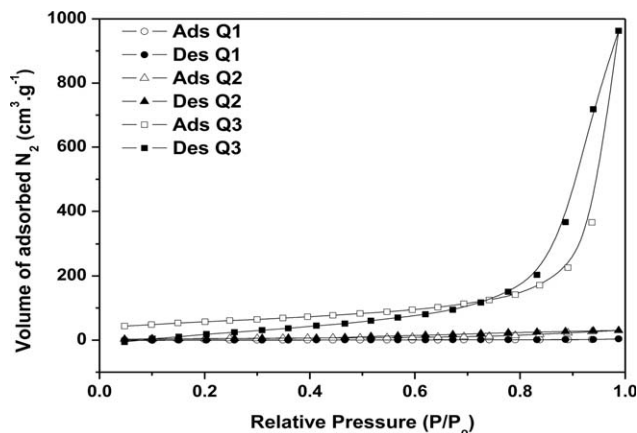


FIG. 7. Nitrogen physisorption isotherms of samples Q1, Q2, and Q3.

carbonization of the material. In fact, according to the literature on the subject, the higher crystallinity index (I_{cr}) of sample Q3 may also explain its greater weight loss.

As the samples are chemically very similar, the slight differences observed in terms of mass loss and maximum degradation temperature can be attributed to the samples' different values of average molar mass and morphology, as well as to their crystallinity, as mentioned earlier.

Specific Surface Area and Porosity. The drying processes used on the chitosan samples yielded materials with varying surface areas, pore sizes and pore volumes. Based on the information extracted from the adsorption/desorption isotherms shown in Fig. 7 and the data in Table 1, samples Q1 and Q2 have low porosity and a small specific surface area. However, in the case of sample Q2, in addition to the apparent decrease in particle size when compared with Q1 (Fig. 3a and b), the increase in specific surface area (Q1: $1.07 \text{ m}^2 \text{ g}^{-1}$; Q2: $16.7 \text{ m}^2 \text{ g}^{-1}$) is also justified by the increase in surface roughness caused by the rapid elimination of the solvent. Despite the 8.5-fold larger pore volume than Q1, the pores in sample Q2 are small, which is probably due to the torsion the polymer chains underwent during drying, not only at the surface but also inside the particles.

The precipitation of chitosan particles by SAS caused a large increase in the specific surface area of sample Q3 ($202.1 \text{ m}^2 \text{ g}^{-1}$) because it resulted in very fine particles with a large pore volume (32-fold larger than Q2), which tends to favor exposure of the amine groups. Allied to these characteristics, the average size of about 15 \AA favors the access of molecules of kinetic size equivalent to the range of micro/mesopores to the amine groups, potentiating the application of the material in the areas of catalysis and adsorption, for example.

CONCLUSIONS

It is concluded that the chitosan drying step can interfere decisively in its molecular weight. Drying by supercritical CO_2 reduced the molar mass of chitosan more than 10-fold when compared to traditional oven drying. The material obtained showed marked changes in particle characteristics: significant increase in pore volume and specific surface area, with no structural modification whatsoever. This work makes an significant

contribution to the theme, demonstrating that the supercritical CO_2 drying method is a promising chitosan depolymerization technique.

ACKNOWLEDGMENT

The authors thank Prof. Dr. Sérgio P. Campana Filho (IQSC/USP) for the viscometry assays.

REFERENCES

1. J.E. Santos, E.R. Dockal, and E.T.G. Cavalheiro, *Carbohydr. Polym.*, **60**, 277 (2005).
2. Y. Zhang, M. Huo, J. Zhou, D. Yu, and Y. Wu, *Carbohydr. Polym.*, **77**, 231 (2009).
3. K.V. Harish-Prashanth and R. N. Tharanathan, *Trends Food Sci. Technol.*, **18**, 117 (2007).
4. C. Shen, Y. Shen, Y. Wen, H. Wang, and W. Liu, *Water Res.*, **45**, 5200 (2011).
5. FAO—Fisheries and Aquaculture Department, *World Review of Fisheries and Aquaculture*, Food and Agriculture Organization of the United Nations, Rome, 77 (2012).
6. A. Tolaimate, J. Desbrieres, M. Rhazia, and A. Alaguic, *Polymer*, **44**, 7939 (2003).
7. R. Jayakumar, K.P. Chennazhi, R.A.A. Muzzarelli, H. Tamura, S.V. Nair, and N. Selvamurugan, *Carbohydr. Polym.*, **79**, 1 (2010).
8. A.B. Vishu-Kumar, M.C. Varadaraj, R.G. Lalitha, and R.N. Tharanathan, *Biochim. Biophys. Acta*, **1670**, 137 (2004).
9. Y. Maeda and Y. Kimura, *J. Nutr.*, **134**, 945 (2004).
10. Z. Jia and D. Shen, *Carbohydr. Polym.*, **49**, 393 (2002).
11. W. Yue, P. Yao, and Y. Wei, *Polym. Degrad. Stabil.*, **94**, 851 (2009).
12. L.M. Batista, C.A. Rosa, and L.A.A. Pinto, *J. Food Eng.*, **81**, 127 (2007).
13. Y. Liu, Y. Zhao, and X. Feng, *Appl. Therm. Eng.*, **28**, 675 (2008).
14. M. Aghbashlo, H. Mobli, S. Rafiee, and A. Madadlou, *Renew. Sustain. Energy Rev.*, **22**, 1 (2013).
15. D. Sanli, S.E. Bozbag, and C. Erkey, *J. Mater. Sci.*, **47**, 2995 (2012).
16. E.F. Costa, F.B. Freire, J.T. Freire, and M.L. Passos, *Dry. Technol.*, **24**, 315 (2006).
17. E. Widjojokusumo, B. Veriansyah, and R. Tjandrawinata, *J. CO₂ Util.*, **119**, 140 (2013).
18. I.C.M. Silva, W.L. Santos, I.C.R. Leal, M.G. Zoghbi, A.C. Feirhmann, V.F. Cabral, E.N. Macedo, and L. Cardozo-Filho, *J. Supercrit. Fluids*, **88**, 134 (2014).
19. A.B. García-Bermejo, A. Cardelle-Cobas, A.I. Ruiz-Matute, F. Montañés, A. Olano, and N. Corzo, *Food Hydrocolloid.*, **29**, 27 (2012).
20. W. Thakhiew, S. Devahastin, and S. Soponronnarit, *J. Food Eng.*, **119**, 140 (2013).
21. M. Jaworska, K. Sakurai, P. Gaudon, and E. Guibal, *Polym. Int.*, **52**, 198 (2003).
22. P.C. Srinivasa, M.N. Ramesh, K.R. Kumar, and R.N. Tharanathana, *J. Food Eng.*, **63**, 79 (2004).
23. M.R. Kasaai, *Carbohydr. Polym.*, **68**, 477 (2007).
24. J.E. Santos, J.P. Soares, E.R. Dockal, and S. Campana-Filho, *Polímeros*, **13**, 242 (2003).

25. H. Struszczyk, *J. Appl. Polym. Sci.*, **33**(1), 177 (1987).
26. A.A. Muzzarelli, Chitin. In H.F. Mark, N.M. Bikales, C.G. Overberger, and G. Menges, Eds., *Encyclopedia of Polymers Science Engineering*, John Wiley, New York, 430 (1985).
27. S. Brunauer, P.H. Emmett, and E. Teller, *J. Am. Chem. Soc.*, **60**, 309 (1938).
28. K. Kurita, S. Mori, Y. Nishiyama, and M. Harata, *Polym. Bull.*, **48**, 159 (2002).
29. A.S. Lisbão, *Estrutura e propriedade dos polímeros*. São Carlos: EdUFSCar, 49 (2012).
30. W.J. Tang, C.X. Wang, and C. Donghua, *Polym. Degrad. Stab.*, **87**, 389 (2005).
31. W.D. Callister, *Ciência e Engenharia de Materiais: Uma Introdução*, 7th ed., LTC, Rio de Janeiro, 364 (2008).
32. G.A. Morris, J. Castile, A. Smith, G.G. Adams, and S.E. Harding, *Polym. Degrad. Stab.*, **94**, 1344 (2009).
33. R. Xing, S. Lius, H. Yu, Z. Gao, P. Wang, and C. Li, *Carbohydr. Res.*, **340**, 2150 (2005).
34. S. Mekahlia, and B. Bouzid, *Phy. Proc.*, **2**, 1045 (2009).
35. E.S.C. Junior and H.S. Mansur, *Química Nova*, **31**, 1460 (2008).
36. J. Brugnerotto, J. Lizardi, F.M. Goycoolea, W. Arguèlles-Monal, J. Desbrieres, and M. Rinaudo, *Polymer*, **42**, 3569 (2001).